

Advection–dispersion mass transport associated with a non-aqueous-phase liquid pool

By MARIOS M. FYRILLAS†

Department of Mechanical and Aerospace Engineering, University of California at San Diego,
La Jolla, CA 92093-0411, USA

(Received 10 May 1999 and in revised form 1 December 1999)

The two-dimensional problem of advection–dispersion associated with a non-aqueous-phase liquid (NAPL) pool is addressed using the boundary element method. The problem is appropriately posed with an inhomogeneous boundary condition taking into consideration the presence of the pool and the impermeable layer. We derive a Fredholm integral equation of the first kind for the concentration gradient along the pool location and compute the average mass transfer coefficient numerically using the boundary-element method. Numerical results are in agreement with asymptotic analytical solutions obtained for the cases of small and large Péclet number (Pe_x). The asymptotic solution for small Pe_x , which is obtained by applying a novel perturbation technique to the integral equation, is used to de-singularize the integral equation. Results predicted by this analysis are in good agreement with experimentally determined overall mass transfer coefficients.

1. Introduction

Environmental consciousness has been augmented in recent years owing to the impact of pollution on the quality of life. One topic of great concern is the contamination of the subsurface by the introduction and movement of non-aqueous-phase liquids (NAPLs), as it presents a threat to the long-term quality of soil and underground water reserves. Most of the NAPLs are organic solvents and petroleum hydrocarbons originating from leaking underground storage tanks, ruptured pipelines, surface spills, hazardous waste landfills and disposal sites. When a NAPL spill which is more dense than water infiltrates the subsurface environment, it will continue to migrate downwards leaving behind trapped ganglia until it encounters an impermeable layer. There, it will form a flat source zone or pool with relatively limited spatial extent (Hunt, Sitar & Udell 1988). On the other hand, NAPL pools with densities lower than that of water will, as they approach the saturated region, spread laterally and float on the water table in the form of a pool. Due to their low solubility in water, NAPL pools may lead to long-lasting sources of groundwater contamination (Bradford, Abriola & Rathfelder 1998).

The dissolution of a NAPL pool in a porous medium is modelled as an advection–dispersion equation where the convection velocity is assumed to be uniform and equal to the interstitial velocity of the water (Bear 1972). A fundamental difference between NAPL advection–dispersion models and classical models that characterize

† Present address: Hyperion Systems Engineering Ltd., 23 Ezekia Papaioannou St., Off. 51, CY-1075 Nicosia, Cyprus; email: mfyryllas@cytanet.com.cy.

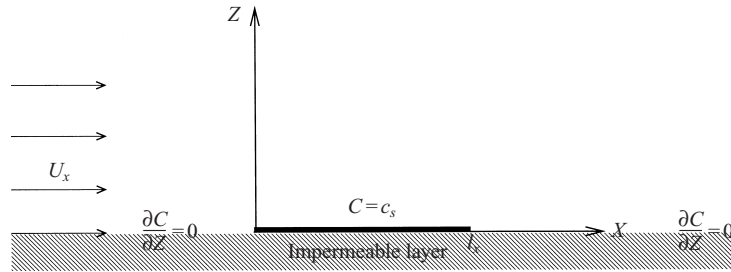


FIGURE 1. Schematic representation of the conceptual physical model along with boundary conditions. Groundwater with unidirectional velocity U_x is flowing over a NAPL pool of length l_x . The concentration over the pool is the saturation concentration c_s , while a no-flux boundary condition is imposed in the area not covered by the pool.

convection–diffusion processes (Leal 1992; Kays & Crawford 1993) is that, in the former case, there is no momentum boundary layer formed.

Although there is a relatively large body of available literature on pool dissolution (Chrysikopoulos, Voudrias & Fyrrillas 1994; Holman & Javandel 1996; Hunt *et al.* 1988; Abriola & Pinder 1985; Seagren, Rittmann & Valocchi 1994; Leij, Toride & van Genuchten 1993; Prakash 1984; Toride, Leij & van Genuchten 1993; to mention a few), it does not address the fundamental problem of pool dissolution in the sense that a homogeneous (Neumann, Dirichlet or a linear combination) boundary condition on the plane of the pool is used. Imposing a Neumann boundary condition requires an *a priori* assumption for the mass flux over the pool while imposing a Dirichlet boundary condition leads to a mass flux over the impermeable layer. More appropriate would be to define the concentration, i.e. a Dirichlet boundary condition, at the pool location and impose no flux, i.e. Neumann boundary condition, in the region not covered by the pool.

In this paper we address precisely this problem using ‘a powerful class of numerical methods, known under the aliases *boundary integral*, *boundary element*, *boundary-integral-equation*, *panel*’ and *Green’s function* methods (Pozrikidis 1997, 1992) which rely on Green’s second identity, or a generalization. We are able to derive a Fredholm integral equation of the first kind for the concentration gradient along the pool location. Analytical expressions are obtained for small and large Péclet numbers (§3), while a collocation boundary-element method using constant functions over each element is used to solve the integral equation numerically (§4). The agreement between numerical results and the asymptotic analytical solutions is quite satisfactory. In §4.1, we compare the results predicted by this analysis with available experimentally determined mass transfer coefficients.

2. Formulation

Consider a single-component NAPL pool which is denser than water and is formed on top of an impermeable layer within a two-dimensional, saturated, homogeneous and isotropic porous medium (figure 1). The steady-state transport of the dissolving contaminant into the aqueous phase under uniform flow conditions is governed by

$$U_x \frac{\partial C(X, Z)}{\partial X} = D_x \frac{\partial^2 C(X, Z)}{\partial X^2} + D_z \frac{\partial^2 C(X, Z)}{\partial Z^2} - \lambda C(X, Z),$$

where λ is the first-order decay coefficient, D_x and D_z are the longitudinal and vertical hydrodynamic dispersion coefficients respectively, and U_x is the average interstitial fluid velocity. The appropriate (inhomogeneous) boundary condition on top of the impermeable layer is

$$\frac{\partial C(X < 0, Z = 0)}{\partial Z} = 0, \quad C(0 \leq X \leq l_x, Z = 0) = c_s, \quad \frac{\partial C(X > l_x, Z = 0)}{\partial Z} = 0,$$

while the far-field conditions are

$$C(\pm\infty, Z) = C(X, \infty) = 0.$$

The problem is non-dimensionalized by scaling lengths with the pool dimension l_x and the concentration by the saturation concentration c_s to obtain the classical dimensionless parameters:

$$Pe_x = \frac{U_x l_x}{D_x}, \quad Pe_z = \frac{U_x l_x}{D_z}, \quad A = \frac{\lambda l_x}{U_x}.$$

The problem takes the form

$$\frac{\partial c(x, z)}{\partial x} = \frac{1}{Pe_x} \frac{\partial^2 c(x, z)}{\partial x^2} + \frac{1}{Pe_z} \frac{\partial^2 c(x, z)}{\partial z^2} - A c(x, z), \quad (2.1)$$

with boundary conditions

$$\frac{\partial c(x < 0, z = 0)}{\partial z} = 0, \quad c(0 \leq x \leq 1, z = 0) = 1, \quad \frac{\partial c(x > 1, z = 0)}{\partial z} = 0,$$

$$c(\pm\infty, z) = c(x, \infty) = 0.$$

The boundary-element formulation is derived in Appendix A and repeated here for ready reference:

$$c(x, z) = -\frac{\sqrt{Pe_x}}{\sqrt{Pe_z \pi}} \int_0^1 \frac{\partial c(x', z' = 0)}{\partial z'} \times \exp[Pe_x/2(x - x')] K_0[\sqrt{(Pe_x/4 + A)} \sqrt{Pe_x(x' - x)^2 + Pe_z z^2}] dx'. \quad (2.2)$$

When evaluated on the plane of the pool ($z = 0$) we obtain a Fredholm integral equation of the first kind for the concentration gradient along the pool location, $0 \leq x \leq 1$,

$$1 = -\frac{\sqrt{Pe_x}}{\sqrt{Pe_z \pi}} \int_0^1 \frac{\partial c(x', z' = 0)}{\partial z'} \times \exp[Pe_x/2(x - x')] K_0[\sqrt{Pe_x(Pe_x/4 + A)} |x' - x|] dx'. \quad (2.3)$$

3. Analysis

In this section we obtain asymptotic solutions in the limit of small and large Pe_x . For simplicity we assume that there is no decay, i.e. $A = 0$ and equation (2.3) simplifies to

$$1 = -\frac{\sqrt{Pe_x}}{\sqrt{Pe_z \pi}} \int_0^1 \frac{\partial c(x', z' = 0)}{\partial z'} \exp[Pe_x/2(x - x')] K_0[Pe_x/2|x' - x|] dx'. \quad (3.1)$$

3.1. Large Pe_x

In the limit of large Pe_x ($Pe_x \rightarrow \infty$) we transform the variables x and x' to $\mathcal{X} = xPe_x/2$ and $\mathcal{X}' = x'Pe_x/2$, respectively. We also introduce the boundary-layer coordinate $\zeta' = z'\sqrt{Pe_z}$ (see Appendix B). Equation (3.1) transforms to

$$1 = -\frac{2}{\pi\sqrt{Pe_x}} \int_0^\infty \frac{\partial c(\mathcal{X}', \zeta' = 0)}{\partial \zeta'} \exp [(\mathcal{X} - \mathcal{X}')] K_0[|\mathcal{X}' - \mathcal{X}|] d\mathcal{X}', \quad (3.2)$$

which suggests that the finite-plate, infinite- Pe_x problem is equivalent to that of a semi-infinite plate. This problem can be easily solved by transforming to parabolic coordinates. We will omit the details as the problem is treated in Greenberg (1978, ex. 26.43, p. 561). In Appendix C (equation C 3) we show that indeed the expression for the flux obtained in the semi-infinite case satisfies integral equation (3.2). Hence in the limit $Pe_x \rightarrow \infty$ the solution is

$$\frac{\partial c(\mathcal{X}', \zeta' = 0)}{\partial \zeta'} = -\sqrt{\frac{Pe_x}{2\pi\mathcal{X}'}}$$

or

$$\frac{\partial c(x, z = 0)}{\partial z} = -\sqrt{\frac{Pe_z}{\pi x}} \quad (3.3)$$

in the original variables. This result can also be obtained by boundary-layer analysis (Appendix B).

3.2. Small Pe_x

When there is no convection and no first-order decay, i.e. $Pe_x = Pe_z = 0$ and $\Lambda = 0$, equation (2.1) reduces to the two-dimensional Laplacian in an infinite domain. This is well known to be an ill-posed problem, the nature of which is clearly demonstrated in the boundary element formulation (equation (2.2)). To address this singular limit of the partial differential equation (2.1), one would probably need to resort to singular perturbation techniques, i.e. matched asymptotic expansions. However, using the boundary element formulation (equations (2.2) and (2.3)) we can address this limit in an elegant manner. We expand the kernel of integral equation (3.1), which we are tempted to identify as the inner problem, to zeroth-order in Pe_x to obtain the weakly singular integral equation

$$1 = \frac{\sqrt{Pe_x}}{\sqrt{Pe_z}\pi} \int_0^1 \frac{\partial c(x', z' = 0)}{\partial z'} \left(\gamma + \ln \left[\frac{Pe_x}{4} \right] + \ln [|x - x'|] \right) dx'.$$

In view of identity (C 1) we assume a solution of the form

$$\frac{\partial c(x', z' = 0)}{\partial z'} = \frac{a_0}{\sqrt{x'(1-x')}},$$

which reduces the integral equation to an algebraic equation with solution

$$a_0 = \sqrt{\frac{Pe_z}{Pe_x}} \frac{1}{b},$$

where

$$b = \gamma + \ln \left[\frac{Pe_x}{16} \right].$$

In Appendix D, the perturbation analysis is continued to higher order to obtain

the following result for the concentration gradient along the pool ($0 \leq x \leq 1$), valid for small Pe_x :

$$\frac{\partial c(x, z = 0)}{\partial z} = \frac{\sqrt{Pe_z}}{\sqrt{Pe_x}} \left(\frac{1}{b} - \frac{Pe_x(1+b)}{4b} (1-2x) \right) \frac{1}{\sqrt{x(1-x)}} + \text{h. o. terms.} \quad (3.4)$$

4. Numerical results

In this section we perform a numerical evaluation of the concentration gradient by applying the boundary element method to the integral equation (2.3). In general, the solution of integral equations of the first kind is susceptible to oscillations due to ill-conditioning of the influence matrix (Pozrikidis 1992, 1997). In the present analysis, the integral equation (2.3) exhibits regular behaviour.

The numerical method used is the collocation boundary element method (Pozrikidis 1992, 1997), where the local basis functions are step functions, i.e. the boundary ($0 \leq x \leq 1$) is discretized into a collection of straight segments (boundary elements), and it is assumed that the unknown function is constant over each element. In view of the results of §3, we expect a singular value for the concentration gradient at the two end points $x = 0, 1$. Hence, we ‘de-singularize’ integral equation (3.1) by defining the function f in the following way:

$$f(x) = -\sqrt{\frac{Pe_x}{Pe_z}} \sqrt{x(1-x)} \frac{\partial c(x, z = 0)}{\partial z}.$$

In addition, to minimize numerical error, we rewrite integral equation (2.3) in the following form:

$$\exp[-\frac{1}{2}Pe_x x] = \frac{1}{\pi} \int_0^1 f(x') \frac{\exp[-\frac{1}{2}Pe_x x'] K_0[\sqrt{Pe_x(Pe_x/4 + A)}|x' - x|]}{\sqrt{x'(1-x')}} dx'.$$

The discrete form of this equation is

$$\exp[-\frac{1}{2}Pe_x x_j] = \sum_{i=1}^N f_i A_{ij}, \quad (4.1)$$

where f_i is the constant value of the function $f(x')$ over the i th element and $j = 1, 2, \dots, N$. The influence matrix is defined as

$$A_{ij} = \int_{x_i}^{x_{i+1}} \frac{\exp[-\frac{1}{2}Pe_x x'] K_0[\sqrt{Pe_x(Pe_x/4 + A)}|x' - x_j|]}{\sqrt{x'(1-x')}} dx',$$

where x_i and x_{i+1} are the starting and ending points of the i th element respectively, and x_j is the midpoint of the j th element. The coefficients of matrix \mathbf{A} are computed by Gauss quadratures (Press *et al.* 1989): Gauss–Legendre for the non-singular elements and Gauss–Chebyshev for the singular elements.

The N -system of equations (4.1) is solved by Gaussian elimination (Press *et al.* 1989). Experimentation showed that 100 elements are adequate to obtain satisfactory accuracy for any value of Pe_x . In figure 2 we compare the results of the numerical procedure with the asymptotic results for high and low Pe_x obtained in §3, equations (3.3) and (3.4) respectively. The very good agreement in both limiting cases suggests that this simple numerical technique is quite effective and accurate for any value of Pe_x .

In figure 3 we show numerical results for different Pe_x . As indicated by the finite

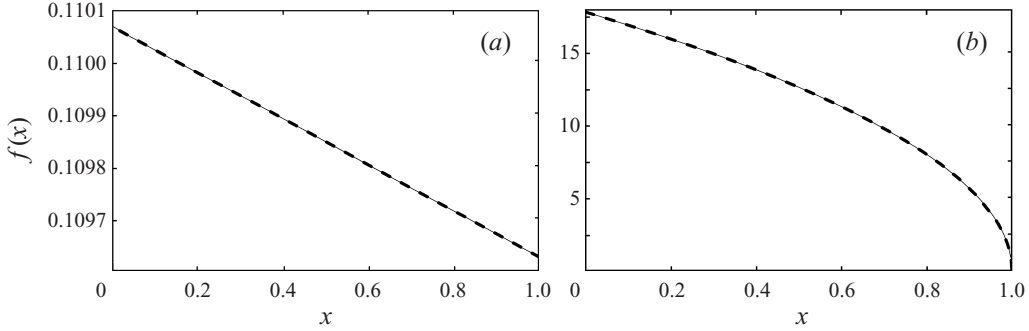


FIGURE 2. Comparison between the asymptotic results (thick-dashed curves) and numerical results (fine-solid curves): (a) $Pe_x = 0.001$ and (b) $Pe_x = 1000$. $A = 0$.

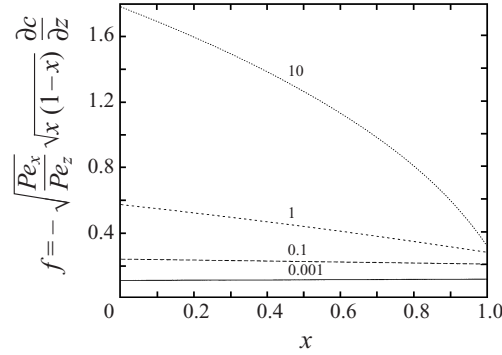


FIGURE 3. Computed values of the function f for the values of Pe_x shown on the figure. $A = 0$.

value of f at $x = 0$ and 1, it is apparent that the singular nature of the concentration gradient at the leading and trailing edges of the pool is present for any finite value of Pe_x , while the singularity at the trailing edge disappears only at infinite Pe_x (§ 3.1).

In figure 4, we show a contour plot of the concentration field at large ($Pe_x = Pe_z = 100$) and small ($Pe_x = Pe_z = 0.1$) Péclet numbers, obtained by substituting the expression for the concentration gradient (§ 3) in equation (2.2) and integrating by Gaussian quadrature. The effect of convection is quite distinct in the two cases: at large Péclet number (convection-dominated mass transport) the contaminant is convected downstream and the diffusion process is restricted to a boundary layer region close to the pool; at small Péclet number (diffusion-dominated mass transport) the effect of convection is only apparent at large distances from the pool, while close to the pool the concentration gradient is almost uniform.

4.1. Average (overall) mass transfer coefficients

The average mass transfer coefficient is defined as (Chrysikopoulos *et al.* 1994; Incropera & DeWitt 1990)

$$\bar{h}_m = -\frac{D_e}{l_x c_s} \int_0^{l_x} \frac{\partial C(X, Z = 0)}{\partial Z} dX = -\frac{D_e}{l_x} \int_0^1 \frac{\partial c(x, z = 0)}{\partial z} dx, \quad (4.2)$$

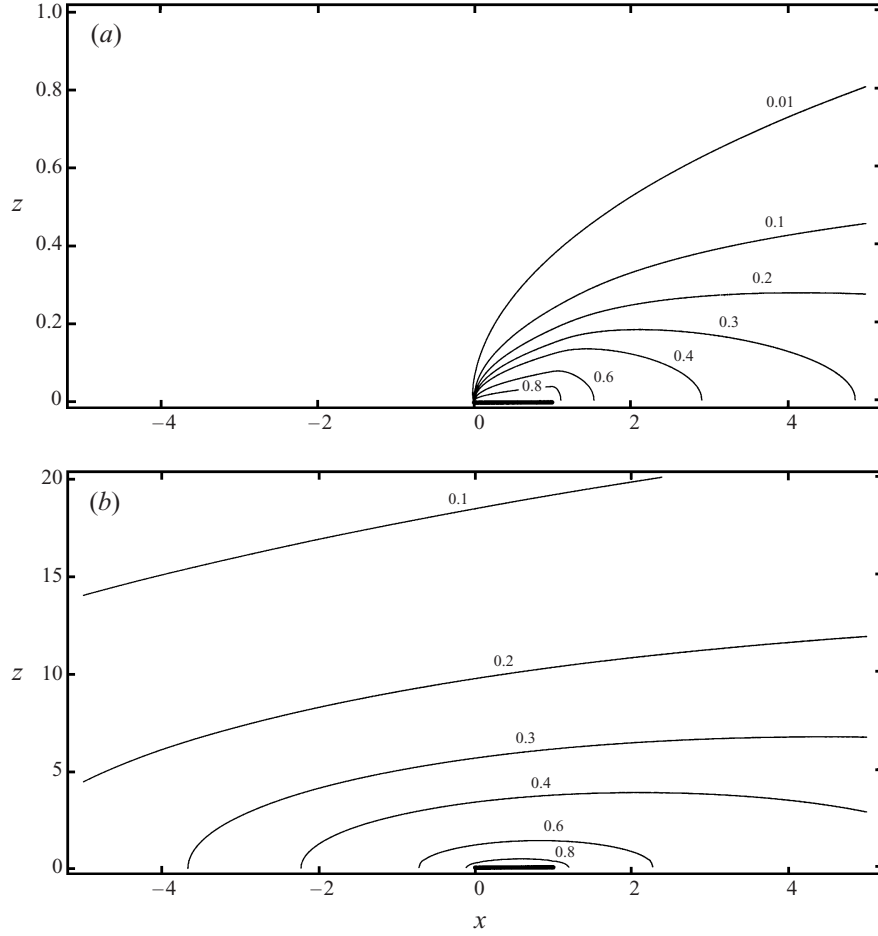


FIGURE 4. A contour plot of the concentration field for $Pe_x = 100$ (a) and $Pe_x = 0.1$ (b). In both calculations $Pe_x = Pe_z$ and $\Lambda = 0$.

where $D_e = D/\tau^*$ is the effective molecular diffusion coefficient; D is the molecular diffusion coefficient and τ^* is the tortuosity. For the two limiting cases of § 3 we obtain

$$\bar{h}_m = -\frac{D_e}{l_x} \sqrt{\frac{Pe_z}{Pe_x}} \frac{\pi}{b} \quad \text{for small } Pe_x \quad (4.3)$$

and

$$\bar{h}_m = \frac{D_e}{l_x} 2\sqrt{\frac{Pe_z}{\pi}} \quad \text{for large } Pe_x. \quad (4.4)$$

In figure 5(a) we compare the Sherwood number (Incropera & DeWitt 1990), defined as

$$\bar{Sh} = \frac{l_x}{D_e} \sqrt{\frac{Pe_x}{Pe_z}} \bar{h}_m, \quad (4.5)$$

and calculated using expressions (4.3) and (4.4) with that obtained from numerical results. As indicated in figure 5(a), for $Pe_x > 10$ expression (4.4) will predict the numerical result quite accurately.

So far, we have not investigated the effect of the decay coefficient (Λ) on the

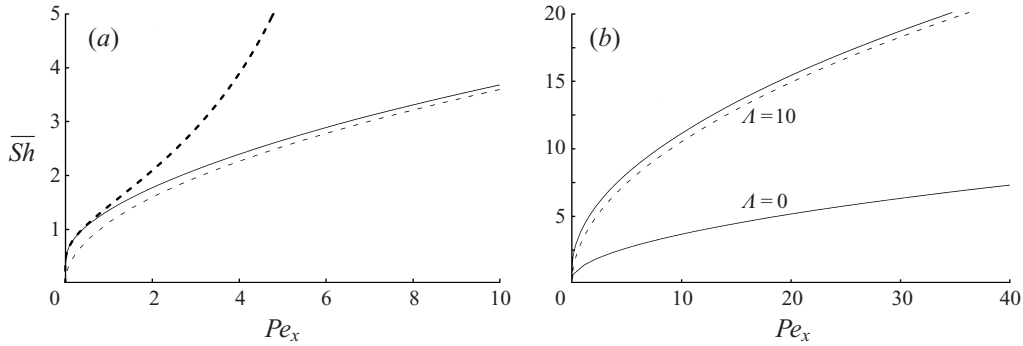


FIGURE 5. Computed values of the Sherwood number, equation (4.5). In (a) ($A = 0$) the thick-dashed curve corresponds to equation (4.3) (small Pe_x) and the thin-dashed curve to equation (4.4) (large Pe_x). The thin solid curve corresponds to numerical results. In (b) the solid curves correspond to numerical results for the values of the decay coefficient (A) shown on the figure. The dashed curve corresponds to the asymptotic result (equation (4.6)) for $A = 10$.

diffusion process. In Appendix B we obtain an expression for the mass transfer coefficient in the limit of high Pe_x :

$$\bar{h}_m = \frac{D_e \sqrt{Pe_z}}{l_x} \left\{ \operatorname{erf}[\sqrt{A}] \left(\sqrt{A} + \frac{1}{2\sqrt{A}} \right) + \frac{e^{-A}}{\sqrt{\pi}} \right\}. \quad (4.6)$$

The asymptotic result (4.6), shown as a dashed curve in figure 5(b), is in good agreement with the numerical result for large Pe_x . Also in figure 5(b) we demonstrate that the reaction rate would enhance the diffusion process and lead to higher mass transfer coefficients. With reaction the concentration field at any point outside the pool is reduced thereby resulting in higher concentration gradients.

Experimental results for mass transfer coefficients are quite limited. In figure 6, results for \bar{h}_m predicted by this work are compared with those obtained experimentally by Lee (1999) in a circular ($l_r = 3.8$ cm) trichloroethylene (TCE) pool dissolution experiment in a homogeneous, fully saturated bench-scale aquifer under various interstitial velocities. To make the comparison, we use l_x corresponding to a square pool with a surface area equal to that of the circular disc, i.e. $l_x = l_r \sqrt{\pi}$. The dispersion coefficients are evaluated using (Bear & Verruijt 1987)

$$D_x = \alpha_L U_x + D_e, \quad D_z = \alpha_V U_x + D_e, \quad (4.7)$$

where α_L and α_V are the longitudinal and vertical dispersivities respectively. Lee (1999) has obtained the following values for the parameters: $D_e = 2.11 \times 10^{-2} \text{ cm}^2 \text{ h}^{-1}$, $\alpha_L = 0.259 \text{ cm}$, and $\alpha_V = 0.019 \text{ cm}$. In figure 7 we show a plot of Pe_x as a function of the interstitial velocity U_x . The resulting \bar{h}_m (solid line in figure 6) is in good agreement with the experimental values. Although it slightly overestimates the mass transfer coefficient, the following rationale leads to the conclusion that two-dimensional predictions should underestimate the mass transfer coefficient. Consider, for example, a square pool in a physical (three-dimensional) experiment. The four sides will contribute significantly to mass transport as the concentration gradient is singular close to the edges. The mass transport from an equal-size square taken from an infinite strip will, however, be less since the concentration gradients at the two fictitious sides (cut from the strip) will be lower. As a justification, in Appendix E we have obtained an exact three dimensional result for the mass transport associated

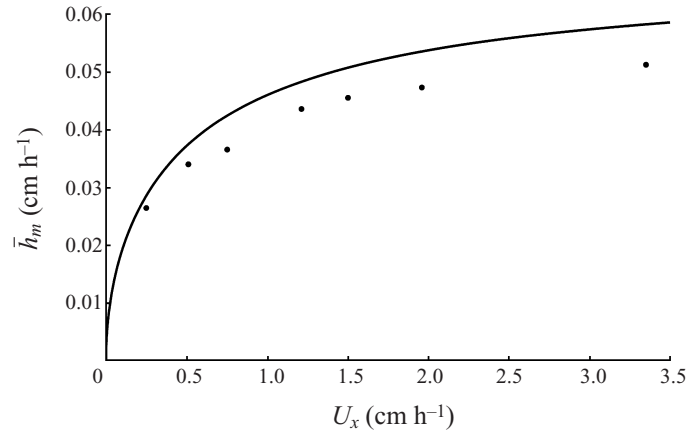


FIGURE 6. Comparison between numerical results (solid line) predicted by this analysis and experimental results (solid points) obtained by Lee (1999). The three-dimensional result obtained in Appendix E (equation (4.8)) gives a value of $\bar{h}_m = 0.007 \text{ cm h}^{-1}$ for $U_x = 0$.

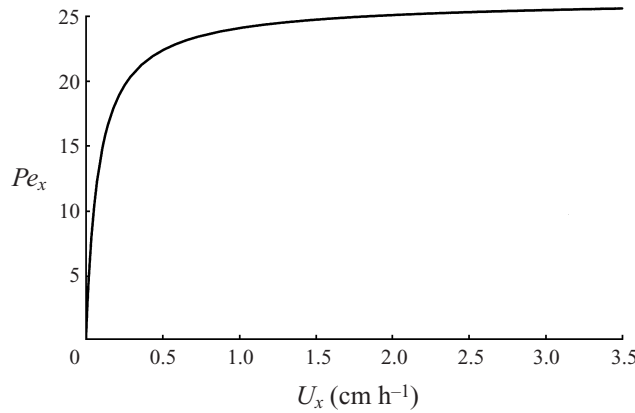


FIGURE 7. Plot of $Pe_x = U_x l_x / (a_L U_x + D_e)$ as a function of the interstitial velocity U_x ; $D_e = 2.11 \times 10^{-2} \text{ cm}^2 \text{ h}^{-1}$, $\alpha_L = 0.259 \text{ cm}$ and $l_x = 3.8\sqrt{\pi} \text{ cm}$. For large U_x , Pe_x reaches the asymptotic value of $l_x/a_L = 26.01$.

with a circular liquid pool with no advection, i.e. in the limit $U_x \rightarrow 0$:

$$\bar{h}_m = \frac{4D_e}{\pi l_r}. \quad (4.8)$$

Although for the two-dimensional case the average mass transfer coefficient is zero, the three-dimensional result predicts a finite mass transfer coefficient $\bar{h}_m = 0.007 \text{ cm h}^{-1}$ (equation (4.8)).

5. Conclusions

We have presented a boundary element formulation and a numerical solution of the problem of advection–dispersion mass transport associated with a NAPL pool. The problem is appropriately modelled by defining the concentration, i.e. Dirichlet boundary condition, at the pool location and imposing no flux, i.e. Neumann boundary condition, in the area not covered by the pool.

We derive a Fredholm integral equation of the first kind for the concentration gradient. Analytical expressions are obtained for small and large Péclet (Pe_x) numbers, while a collocation boundary-element method using constant functions over each element is used to solve the integral equation numerically for any Pe_x . The agreement between numerical results and the two asymptotic analytical solutions is quite satisfactory which suggests that the numerical technique is effective and accurate for any value of Pe_x . There is a fairly good agreement between the present analysis and the experimental data, even though the latter were obtained in a three-dimensional experiment. In the case of no advection, comparison between two-dimensional and three-dimensional analytical results suggests that the former would predict a lower mass transfer coefficient.

The author would like to express his gratitude to Mikis, Fedra, Keiko Nomura and Costas Pozrikidis for their continuous support. The author would also like to thank the referee who pointed out an error in the proof in Appendix C.

Appendix A. Boundary-element formulation

The transformations of the dependent variable

$$c(x, z) = W(x, z) \exp \left[\frac{xPe_x}{2} \right]$$

and of the independent variables

$$x = \frac{\chi}{\sqrt{Pe_x}}, \quad z = \frac{\zeta}{\sqrt{Pe_x}},$$

reduces equation (2.1) to the two-dimensional modified Helmholtz equation:

$$\nabla_{(\chi, \zeta)}^2 W - \left(\frac{1}{4}Pe_x + A\right)W = 0, \quad (\text{A } 1)$$

with boundary conditions

$$\begin{aligned} \frac{\partial W(\zeta = 0)}{\partial \zeta} &= 0, & \chi < 0, \\ W(\zeta = 0) &= \exp \left[-\frac{\chi\sqrt{Pe_x}}{2} \right], & 0 \leq \chi \leq \sqrt{Pe_x}, \\ \frac{\partial W(\zeta = 0)}{\partial \zeta} &= 0, & \chi > \sqrt{Pe_x}, \end{aligned}$$

and the constraint that the concentration field decays to zero far away from the pool.

Then, as a simple generalization of Green's theorem (Arfken 1985), we have

$$\int_D (G\mathcal{L}W - W\mathcal{L}G) d\tau = \int_{\partial D} (G\nabla W - W\nabla G) \cdot d\sigma,$$

where \mathcal{L} is the modified Helmholtz operator $\nabla_{(\chi', \zeta')}^2 - (Pe_x/4 + A)$, the domain D is the upper half-plane and the boundary (∂D) the line $\zeta' = 0$. By choosing G to be the Green's function that is symmetric about $\zeta' = 0$, i.e.

$$\mathcal{L}G = -\delta(\chi' - \chi, \zeta' - \zeta), \quad (\text{A } 2)$$

$$\frac{\partial G(\zeta' = 0)}{\partial \zeta'} = 0,$$

we obtain the boundary element formulation of problem (A 1)

$$W(\chi, \zeta) = - \int_0^{\sqrt{Pe_x}} \frac{\partial W(\chi', \zeta' = 0)}{\partial \zeta'} G(\chi', \chi, \zeta' = 0, \zeta) d\chi'. \quad (\text{A } 3)$$

The Green's function satisfying equation (A 2) can be obtained using the method of images (Greenberg 1978)

$$G = \frac{1}{2\pi} K_0[\sqrt{(Pe_x/4 + \Lambda)}\sqrt{(\chi' - \chi)^2 + (\zeta' - \zeta)^2}] \\ + \frac{1}{2\pi} K_0[\sqrt{(Pe_x/4 + \Lambda)}\sqrt{(\chi' - \chi)^2 + (\zeta' + \zeta)^2}],$$

where K_0 represents the modified Bessel function of the second kind of order 0.

Expressing equation (A 3) in the original variables we obtain

$$c(x, z) = - \frac{\sqrt{Pe_x}}{\sqrt{Pe_z}\pi} \int_0^1 \frac{\partial c(x', z' = 0)}{\partial z'} \\ \times \exp[-Pe_x/2(x' - x)] K_0[\sqrt{(Pe_x/4 + \Lambda)}\sqrt{Pe_x(x' - x)^2 + Pe_z z^2}] dx'.$$

Appendix B. Boundary-layer approximation

In the limit of large Péclet number ($Pe_x \gg 1$) we introduce the boundary-layer coordinate $\zeta = z\sqrt{Pe_z}$, and expand the concentration field (c) in powers of $1/Pe_x$.

To leading order we obtain the boundary-layer problem

$$\frac{\partial c(x, \zeta)}{\partial x} = \frac{\partial^2 c(x, \zeta)}{\partial \zeta^2} - \Lambda c(x, \zeta). \quad (\text{B } 1)$$

Considering the parabolic nature of the problem (there is no diffusion in the x -direction) the boundary conditions are also simplified:

$$c(x = 0, \zeta) = 0, \quad c(x, \zeta = 0) = 1, \quad c(x, \infty) = 0. \quad (\text{B } 2)$$

The problem can be solved by taking Laplace transforms with respect to the variable x . The final result is

$$c(x, \zeta) = \frac{e^{\zeta\sqrt{\Lambda}}}{2} \operatorname{erfc}\left[\frac{\zeta + 2x\sqrt{\Lambda}}{2\sqrt{x}}\right] + \frac{e^{-\zeta\sqrt{\Lambda}}}{2} \operatorname{erfc}\left[\frac{\zeta - 2x\sqrt{\Lambda}}{2\sqrt{x}}\right]. \quad (\text{B } 3)$$

When $\Lambda = 0$ we obtain the classical result $c(x, \zeta) = \operatorname{erfc}[\zeta/(2\sqrt{x})]$.

The average mass transfer coefficient is obtained by (see § 4.1)

$$\bar{h}_m = - \frac{De\sqrt{Pe_z}}{l_x} \int_0^1 \frac{\partial c(x, \zeta = 0)}{\partial \zeta} dx. \quad (\text{B } 4)$$

Differentiating equation (B 3) with respect to ζ , taking the limit $\zeta \rightarrow 0$ we obtain

$$\frac{\partial c}{\partial \zeta}(c, \zeta = 0) = -\sqrt{\Lambda} \operatorname{erf}[\sqrt{\Lambda}x] - \frac{e^{-\Lambda x}}{\sqrt{\pi x}}.$$

Substituting above expression into equation (B 4), we obtain the following expression for the mass transfer coefficient:

$$\bar{h}_m = \frac{De\sqrt{Pe_z}}{l_x} \left\{ \operatorname{erf}[\sqrt{\Lambda}] \left(\sqrt{\Lambda} + \frac{1}{2\sqrt{\Lambda}} \right) + \frac{e^{-\Lambda}}{\sqrt{\pi}} \right\},$$

which simplifies to the classical result

$$\bar{h}_m = \frac{2D_e\sqrt{Pe_z}}{l_x\sqrt{\pi}},$$

when $A = 0$.

Appendix C. Useful integrals

For $0 \leq x \leq 1$ we have

$$\int_0^1 \frac{\ln(|x-x'|)}{\sqrt{x'(1-x')}} dx' = -\pi \ln(4) \quad (C1)$$

$$\int_0^1 \frac{x' \ln(|x-x'|)}{\sqrt{x'(1-x')}} dx' = -\pi x + \frac{\pi}{2} - \pi \ln(2). \quad (C2)$$

For $0 \leq x < \infty$ we have

$$\int_0^\infty \frac{e^{(x-x')} K_0(|x-x'|)}{\sqrt{x'}} dx' = \frac{\pi\sqrt{\pi}}{\sqrt{2}}. \quad (C3)$$

The first two integrals (C1) and (C2) can be obtained by an appropriate change of variables in the integrals listed in Magnus & Oberhettinger (1949) and Magnus, Oberhettinger & Soni (1966). For a more rigorous approach we suggest Porter & Stirling (1990).

The last integral (C3) is not listed; in what follows we offer an indirect proof, i.e. we assume that is true and show that it leads to consistent results. Two integrals that would be useful in proving (C3) are

$$\int_0^\infty \frac{e^{-\theta'} K_0(\theta')}{\sqrt{\theta'}(x+\theta')} d\theta' = \frac{\pi e^x K_0(x)}{\sqrt{x}} \quad (C4)$$

and

$$\int_0^\infty \frac{e^{-\theta'} K_0(\theta')}{\sqrt{\theta'}} d\theta' = \frac{\pi\sqrt{\pi}}{2}. \quad (C5)$$

The first integral is listed in Gradshteyn & Ryzhik (1994, 6.624), while the second can be obtained by multiplying the first by x and taking the limit $x \rightarrow \infty$. To proceed, we define the variable $\theta = x - x'$ and split integral (C3) into the two regions $(-\infty, 0)$ and $(0, x)$:

$$\int_0^\infty \frac{e^{-\theta} K_0(\theta)}{\sqrt{x+\theta}} d\theta + \int_0^x \frac{e^\theta K_0(\theta)}{\sqrt{x-\theta}} d\theta = \frac{\pi\sqrt{\pi}}{\sqrt{2}},$$

where in the first integral we have transformed θ to $-\theta$. We re-write the integral in the form

$$\int_0^x \frac{\phi(\theta)}{\sqrt{x-\theta}} d\theta = \int_0^\infty \frac{e^{-\theta} K_0(\theta)}{\sqrt{\theta}} d\theta - \int_0^\infty \frac{e^{-\theta} K_0(\theta)}{\sqrt{x+\theta}} d\theta, \quad (C6)$$

where we have substituted the integral (C5) for $\pi\sqrt{\pi/2}$, and we have defined $\phi(\theta) \equiv e^\theta K_0(\theta)$. Abel's integral equation:

$$G(x) - G(0) = \int_0^x (x-y)^{-\alpha} \phi(y) dy$$

has the solution (Magnus & Oberhettinger 1949)

$$\phi(y) = \frac{\sin(\alpha\pi)}{\pi} \int_0^y (y-x)^{\alpha-1} \frac{dG(x)}{dx} dx.$$

Solving equation (C 6) according to this, we obtain

$$\phi(x) = \frac{1}{2\pi} \int_0^x \int_0^\infty \frac{e^{-\theta'} K_0(\theta')}{(\theta + \theta')^{3/2} \sqrt{x-\theta}} d\theta' d\theta.$$

Switching the order of integration and performing the integral with respect to θ results in

$$\phi(x) = \frac{\sqrt{x}}{\pi} \int_0^\infty \frac{e^{-\theta'} K_0(\theta')}{\sqrt{\theta'}(x+\theta')} d\theta'. \quad (C 7)$$

Simplifying this expression using integral (C 4) we obtain the result $\phi(x) = e^x K_0(x)$. QED.

Appendix D. Higher-order correction in $Pe_x \rightarrow 0$

Continuing to higher order in Pe_x , we expand the kernel in integral equation (3.1) to first order and, consequently, assume a solution for the concentration gradient of the form

$$\frac{\partial c(x', z' = 0)}{\partial z'} = \frac{a_0 + a_1(x')}{\sqrt{x'(1-x')}},$$

where a_1 is of higher order compared to a_0 . The problem associated with a_0 was addressed in § 3.2. The integral equation associated with a_1 is

$$\begin{aligned} & \int_0^1 \frac{a_1(x')}{\sqrt{x'(1-x')}} \left(\gamma + \ln \left[\frac{Pe_x}{4} \right] + \ln [|x-x'|] \right) dx' \\ &= a_0 Pe_x \int_0^1 \frac{(x'-x)(\gamma + \ln [Pe_x/4] + \ln [|x-x'|])}{2\sqrt{x'(1-x')}} \\ &= \frac{\sqrt{Pe_x Pe_z} \pi (1+b)}{4b} (1-2x), \end{aligned}$$

where b was defined in § 3.2.

In view of identities (C 1) and (C 2) we assume a solution of the form

$$a_1(x') = a_1^0 + a_1^1 x',$$

which reduces the integral equation to an algebraic system of equations, for the unknowns a_1^0 and a_1^1 , by setting the coefficients of x^0 and x^1 equal to zero. We obtain the results

$$a_1^0 = -\frac{\sqrt{Pe_z Pe_x} (1+b)}{4b}, \quad a_1^1 = \frac{\sqrt{Pe_z Pe_x} (1+b)}{2b}.$$

Appendix E. Laplace equation over a circular pool

Consider three-dimensional diffusion mass transfer from a circular pool with no convection. The concentration field satisfies the Laplace equation

$$\nabla^2 c = \frac{\partial^2 c}{\partial x^2} + \frac{\partial^2 c}{\partial y^2} + \frac{\partial^2 c}{\partial z^2} = 0,$$

with boundary conditions

$$c(x^2 + y^2 \leq 1, z = 0) = 1,$$

and that c decays to zero in the far field. We have used the radius of the pool (l_r) as the characteristic length for non-dimensionalization and that for no advection the dispersion coefficients are equal, i.e. $D_x = D_y = D_z$ (equations (4.7)). A more natural coordinate system to address this problem is the oblate spheroidal (Happel & Brenner 1965; Landau & Lifshitz 1960) which is related to the Cartesian by

$$x = \cosh \xi \sin \eta \cos \phi, \quad y = \cosh \xi \sin \eta \sin \phi, \quad \text{and} \quad z = \sinh \xi \cos \eta.$$

It is easy to realize that ξ is a similarity transformation and the Laplace equation simplifies to

$$\frac{d}{d\xi} \left[\cosh \xi \frac{dc}{d\xi} \right] = 0,$$

with boundary conditions

$$c(\xi = 0) = 1, \quad \text{and} \quad c(\xi \rightarrow \infty) = 0.$$

The solution can be readily found to be

$$c(\xi) = 1 - \frac{4}{\pi} \tan^{-1} \left[\tanh \frac{\xi}{2} \right],$$

which leads to the following expression for the concentration gradient:

$$\frac{\partial c}{\partial z}(z = 0, x^2 + y^2 \leq 1) = -\frac{2}{\pi \sqrt{1 - (x^2 + y^2)}}.$$

The averaged mass transfer coefficient is given by

$$\bar{h}_m = \frac{4D_e}{\pi l_r} \int_0^1 \frac{r dr}{\sqrt{1 - r^2}} = \frac{4D_e}{\pi l_r}.$$

REFERENCES

- ABRIOLA, L. M. & PINDER, G. F. 1985 A multiphase approach to the modeling of porous media contamination by organic compounds: 1. Equation development. *Water Resour. Res.* **21**, 11–18.
- ARFKEN, G. 1985 *Mathematical Methods for Physicists*. Academic.
- BEAR, J. 1972 *Dynamics of Fluids in Porous Media*. Dover.
- BEAR, J. & VERRUIJT, A. 1987 *Modeling Groundwater Flow and Pollution*. D. Reidel.
- BRADFORD, S. A., ABRIOLA, L. M. & RATHFENDER, K. 1998 Flow and entrapment of dense non-aqueous phase liquids in physically and chemically heterogeneous aquifer formations. *Adv. Water Resour.* **22**, 117–132.
- CHRYSIKOPOULOS, C. V., VOUDRIAS, E. A. & FYRILLAS, M. M. 1994 Modeling of contaminant transport resulting from dissolution of nonaqueous phase liquid pools in saturated porous media. *Transport in Porous Media* **16**, 125–145.
- GRADSHTEYN, I. S. & RYZHIK, I. M. 1994 *Tables of Integrals Series and Products*. Academic.
- GREENBERG, M. D. 1978 *Foundations of Applied Mathematics*. Prentice-Hall.
- HAPPEL, J. & BRENNER, H. 1965 *Low Reynolds Number Hydrodynamics*. Prentice-Hall.
- HOLMAN, H.-Y. N. & JAVANDEL, I. 1996 Evaluation of transient dissolution of slightly water-soluble compounds from a light nonaqueous phase liquid pool. *Water Resour. Res.* **32**, 915–923.
- HUNT, J. R., SITAR, N. & UDELL, K. S. 1988 Nonaqueous phase liquid transport and cleanup, 1. Analysis of Mechanisms. *Water Resour. Res.* **24**, 1247–1258.

- INCROPERA, F. P. & DEWITT, D. P. 1990 *Fundamentals of Heat and Mass Transfer*. John Wiley & Sons.
- KAYS, W. M. & CRAWFORD, M. E. 1993 *Convective Heat and Mass Transfer*. McGraw-Hill.
- LANDAU, L. D. & LIFSHITZ, E. M. 1960 *Electrodynamics of Continuous Media*. Pergamon.
- LEAL, L. G. 1992 *Laminar Flow and Convective Transport Processes*. Butterworth-Heinemann.
- LEE, K. Y. 1999 Dissolution of nonaqueous phase liquid pools in saturated porous media. PhD Dissertation, University of California, Irvine.
- LEIJ, F. J., TORIDE, N. & GENUCHTEN, M. TH. VAN 1993 Analytical solutions for non-equilibrium solute transport in three-dimensional porous media. *J. Hydrol.* **151**, 193–228.
- MAGNUS, W. & OBERHETTINGER, F. 1949 *Formulas and Theorems for the Functions of Mathematical Physics*. Chelsea Publishing Company, New York.
- MAGNUS, W., OBERHETTINGER, F. & SONI, R. P. 1966 *Formulas and Theorems for the Special Functions of Mathematical Physics*. Springer.
- PORTER, D. & STIRLING, D. S. G. 1990 *Integral Equations: A Practical Treatment, from Spectral Theory to Applications*. Cambridge University Press.
- POZRIKIDIS, C. 1992 *Boundary Integral and Singularity Methods for Linearized Viscous Flow*. Cambridge University Press.
- POZRIKIDIS, C. 1997 *Introduction to Theoretical and Computational Fluid Dynamics*. Oxford University Press.
- PRAKASH, A. 1984 Ground-water contamination due to transient sources of pollution. *J. Hydraul. Engng* **110**, 1642–1658.
- PRESS, W. H., FLANNERY, B. P., TEUKOLSKY, S. A. & VETTERING, W. T. 1989 *Numerical Recipes: The Art of Scientific Computing*. Cambridge University Press.
- SEAGREN, E. A., RITTMANN, B. E. & VALOCCHI, A. J. 1994 Quantitative evaluation of the enhancement of NAPL-pool dissolution by flushing and biodegradation. *Environ. Sci. Technol.* **28**, 833–839.
- TORIDE, N., LEIJ, F. J. & GENUCHTEN, M. TH. VAN 1993 A comprehensive set of analytical solutions for nonequilibrium solute transport with first-order decay and zero-order production. *Water Resour. Res.* **29**, 2167–2182.